https://doi.org/10.3311/PPee.42204

Periodica Polytechnica Electrical Engineering and Computer Science

Hybrid and Hexagonal Planar Arrays with Discrete Ring-based Amplitude Distributions for Sidelobe Minimization

Jafar Ramadhan Mohammed[1*]

[1] College of Electronic Engineering, Ninevah University, Al Majmoaa Street, 41002 Mosul, Iraq
[*] Corresponding author, e-mail: jafar.mohammed@uoninevah.edu.iq

Received: 11 September 2025, Accepted: 11 December 2025, Published online: 18 December 2025

Abstract

Hexagonal planar arrays are useful in radar, sonar, and wireless communications due to their ability to provide complete coverage in the azimuth plane. On the other hand, hybrid arrays that combine two different array structures, like a small central square subarray surrounded by a number of rings, are capable of providing better performance than the conventional array architectures. This paper introduces two new planar array structures that are efficiently optimized to best cope with these aforementioned applications. The first proposed design is a planar array with hexagonal structure based on discrete hexagonal-ring amplitude distributions, while the second design structure is the hybrid array architecture with a small central square subarray surrounded by a number of elements in the shape of a ring. The idea of first design structure is to re-represent the conventional element-based excitation amplitudes by discrete hexagonal-based excitation amplitudes in which they are ordered in descending from the center to the array edges. By this way, the amplitude excitations of the array elements become more compatible and practicable with the needed real-life discrete RF attenuators or amplifiers that are used for configuring the targeted excitation amplitudes. Moreover, the discrete hexagonal-based excitation amplitudes need a simpler feeding network than its element-based counterpart, thus, the array cost and complexity are greatly reduced. An optimization scheme based on a genetic algorithm is used to optimize these two proposed array structures to achieve ultra-low sidelobe levels while preserving mainlobe directivity. Simulation results confirm the effectiveness of the proposed array structures.

Keywords

hexagonal planar array, hybrid arrays, sidelobe suppression, array pattern synthesis, genetic algorithm

1 Introduction

Generally, antenna arrays with circular geometries or ring-based planar subarrays are widely employed in radar [1], satellite communication [2], and sonar systems [3] due to their ability to provide 360° azimuthal coverage. Its principle can be also applied in microphone arrays [4], acoustic echo [5], and biomedical applications [6]. However, one of the challenges in the synthesis of a circular array is the suppression of undesirable sidelobes without excessively broadening the main beam and maintaining the array directivity undistorted. Classical solutions include the use of some tapers such as Dolph–Chebyshev and Taylor distributions, which achieve specified sidelobe levels in linear arrays. The Kaiser window, derived from prolate spheroidal functions, has proven to be a versatile tapering function for linear and planar arrays due to its adjustable trade-off between mainlobe width and sidelobe level [7, 8].

Generally, non-uniform excitation tapers such as Dolph–Chebyshev arrays achieve equal-ripple sidelobe behavior, while Taylor distributions allow controlled sidelobe decay. Much published research has extensively addressed synthesis problems in one-dimensional linear and two-dimensional rectangular planar arrays. However, circular planar arrays pose additional challenges due to element placement on concentric rings and non-uniform spacing. Thus, some recent works have explored evolutionary algorithms, convex optimization, and heuristic tapers to suppress sidelobes in circular geometries [9–11]. Such array geometry has been found in biomedical applications, direction-of-arrival estimation, and astronomy [12–15]. To simplify the feeding network complexity, clustered arrays with various geometrical shapes have been also presented [16–19].

Cite this article as: Mohammed, J. R. "Hybrid and Hexagonal Planar Arrays with Discrete Ring-based Amplitude Distributions for Sidelobe Minimization", Periodica Polytechnica Electrical Engineering and Computer Science, 2025. https://doi.org/10.3311/PPee.42204

This paper, first, extends the Kaiser approach to circular arrays and presents an optimization framework to achieve optimum low sidelobe levels. It develops the principle of continuous Kaiser distribution that was used in linear arrays to be applicable for circular apertures and maps it to discrete-hexagonal-based amplitude distribution shape which is more practical from implementation point of view. Further, the author combine closed form tapering with a small parameter optimization for geometry and window parameter β. The main contributions in this design are as follows: the continuous circular aperture with Kaiser taper was efficiently transformed to discrete hexagonal-based Kaiser taper. The design parameters β, ring radii R_m, ring populations N_m and other spacing constraints are optimized to get minimum sidelobe level while preserving the array directivity. Finally, a two stage optimization solver such as genetic algorithm (GA) and convex least squares (LS) was used to find the optimum excitation weights under discrete hexagonal-rings with the same excitation amplitude among all elements that belong to a certain ring.

In the second proposed array, a hybrid structure that combines between two different arrays like a small central square subarray with surrounded rings is suggested. This hybrid array is capable of providing better performance than the conventional planar array architectures. It should be mentioned that this is the first time to introduce such a hybrid array geometry which opens a new horizon for the hybrid planar array geometries.

2 The hexagonal planar array structure

Consider a continuous circular aperture with radius R. The author assume a continuous radial Kaiser taper for $0 \le r \le R$:

$$w(r,R) = \frac{I_o\left\{\beta\sqrt{1-(r/R)^2}\right\}}{I_o(\beta)}, \tag{1}$$

where I_o is the zero-order modified Bessel function, $w(0) = 1$, $w(R) = I_o(0)/I_o(\beta) = 1/I_o(\beta)$ and β is the design parameter that controls the trade-off where large value corresponds to lower sidelobes and wider main beam. The continuous Kaiser taper is shown in Fig. 1 (a). To find the corresponding discrete hexagonal-based taper as shown in Fig. 1 (b), consider a hexagonal planar array with a number of concentric hexagonal-rings $m = 1, 2, \ldots, M$. Let R_m be the ring radius, N_m be the ring population (i.e., the number of array elements in each ring), $\varnothing_{m,n}$ element angles in azimuth plane, (m,n) is the element index, and $R_{m,n}$ is the element position in the array:

$$r_{m,n} = \begin{bmatrix} R_m \cos(\varnothing_{m,n}) \\ R_m \sin(\varnothing_{m,n}) \end{bmatrix}. \tag{2}$$

Further let us assume the discrete complex weight of the ring-based element excitation amplitude is $w_{m,n}$. For such a planar array, the far-field array pattern $A(\varnothing,\theta)$ relative to the broadside (z-axis) can be written as [20]:

$$A(\varnothing,\theta) = \sum_{m=0}^{M}\sum_{n=0}^{N_m} w_{m,n} e^{jk\left(x_{m,n}\sin\theta\cos\varnothing + y_{m,n}\sin\theta\sin\varnothing\right)}, \tag{3}$$

where $k = 2\pi/\lambda$ is the wave number, λ is the wave length, and θ, $\varnothing$ are the elevation and azimuth angles respectively. Clearly, the design variables β, ring radii R_m, ring populations N_m and $w_{m,n}$ can be optimized in two-stage optimization process to obtain minimum sidelobe level while preserving the array directivity.

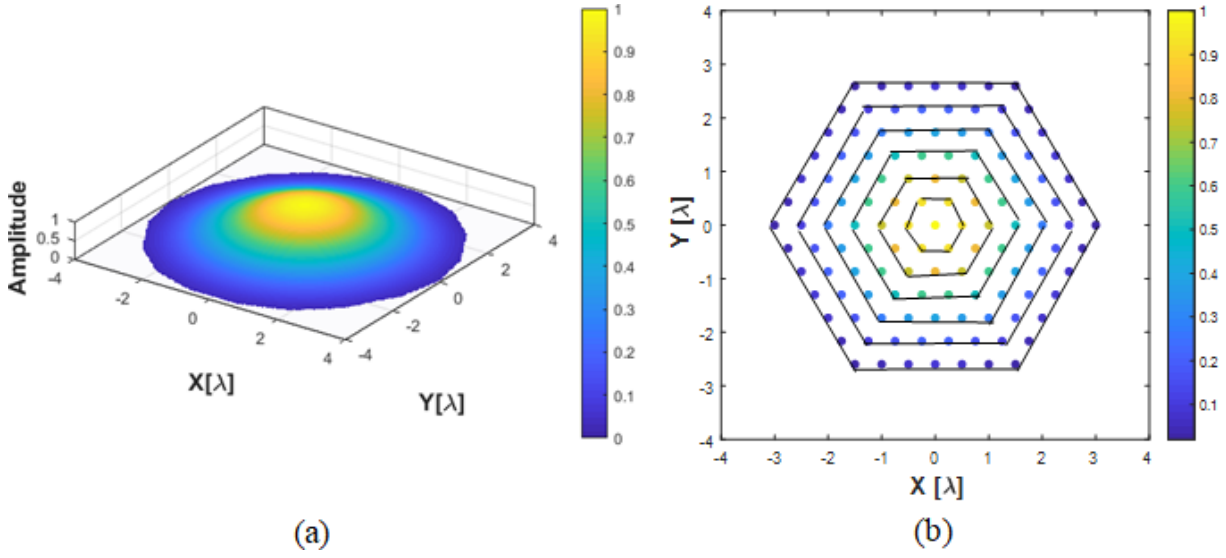

Fig. 1 Continuous (a) and discrete (b) hexagonal tapers

2.1 Objective function optimization

Section 2.1 introduces the objective function that is used to minimize the peak sidelobe level (PSL) in dB over the whole visible region (excluding the mainbeam) of the antenna array pattern, while constraining the beam width or maximizing the array directivity. Thus, it can be formulated as:

$$\min_{\beta\{R_m, N_m, \varnothing_{m,n}, w_{m,n}\}} \max_{(\theta,\varnothing)\in\Omega_{\text{SLL}}} 20\log_{10}\frac{|A(\theta,\phi)|}{\max_{\Omega_{\text{SLL}}}|A|}, \tag{4}$$

$$\text{Subject to } R_{m+1} > R_m, R_M \le R_{\max}. \tag{5}$$

The GA optimization was used to find the optimum value for the design variables $\{\beta, R_1, \ldots, R_M, N_1, \ldots, N_M\}$. Now, let us map the continuous Kaiser taper to the discrete hexagonal rings and elements:

$$R_m = R\sqrt{\frac{m}{M}},\ m = 0,1,\ldots,M. \tag{6}$$

Next, assign discrete ring-based amplitude excitations by sampling the continuous radial taper at R_m:

$$\alpha_m = w(R_m,\beta),\ w_{m,n}^{(0)} = \alpha_m e^{j_0}. \tag{7}$$

After optimizing the geometrical design variables $\{\beta, R_1, \ldots, R_M, N_1, \ldots, N_M\}$ by means of a genetic optimization. The hexagonal array geometry becomes fixed. Next the author solve for discrete complex weights that reduce the sidelobe level with minimal deviation from the prior circular-Kaiser taper. A convex least squares was used to optimize the discrete hexagonal-based amplitude distributions:

$$\min_{w} \boldsymbol{A}_{\text{SLL}} w_2^2 + \lambda_r w - w^{(0)}{}_2^2\ s\cdot t\cdot a_{\text{boresight}}^H w = 1, \tag{8}$$

where $\boldsymbol{A}_{\text{SLL}}$ represents the stacks steering vectors over sidelobe angles; $w^{(0)}$ is the prior circular Kaiser taper and λ_r is the least square regularization parameter. The linear equality fixes broadside gain and maintains the main beam undistorted.

2.2 Ring feeding network design of the proposed hexagonal-based amplitude excitations

The feeding network design of the proposed hexagonal planar array with discrete ring-based amplitude excitations is shown in Fig. 2.

In this design, six hexagonal rings were considered as was presented in Fig. 1 (b). The number of array elements in the first ring and upward are 6, 12, 18, 24, 30, 36 elements. Since each hexagonal ring consists of a certain number of elements and they are sharing the same amplitude and phase excitations, thus, the elements of each hexagonal ring are connected to a single radio frequency (RF) digital attenuator and a single digital phase shifter. The central element is left individually, its normalized amplitude is one while its phase is zero, and thus, it is not connected to any attenuator or phase shifter. From this design, it is clear

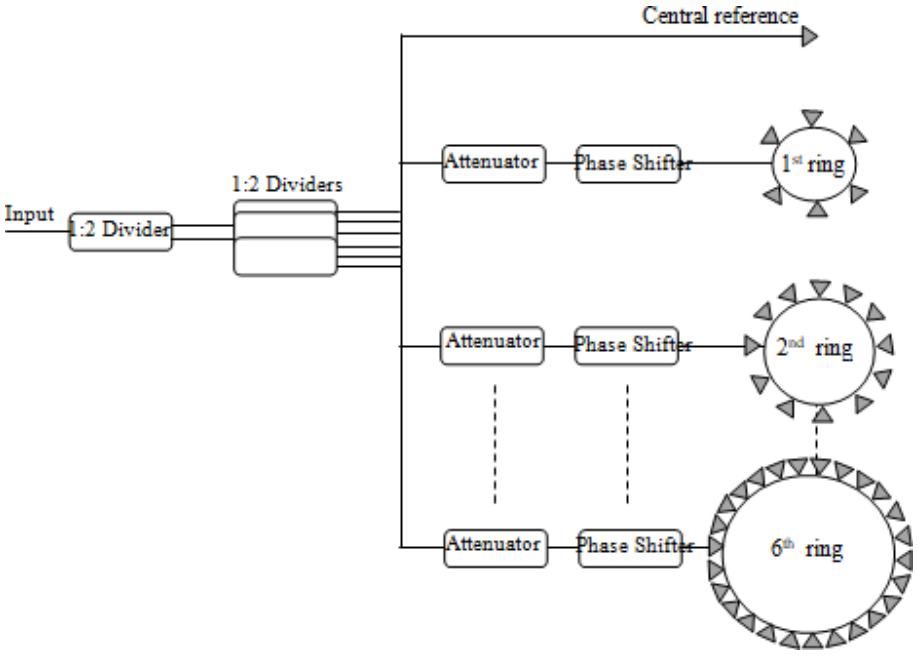

Fig. 2 Feed network design of proposed hexagonal planar array with discrete ring amplitude excitations

that the proposed array needs only 6 digital attenuators and 6 phase shifters, while the conventional element-based amplitude excitations method needs a total number of digital attenuators equal to 126 and the same number of the phase shifters. Such a great reduction in the feeding network complexity makes the proposed discrete hexagonal array practically most efficient and simplest method.

3 The hybrid planar array structure

In Section 3, the author consider a second proposed design geometry of the hybrid array where a fixed central subarray in the form of a small square or rectangular surrounded by a number of array elements whose positions and excitations are need to be optimized to get the minimum sidelobe level in the azimuth plane. The position (x_i, y_i) and weight excitation w_i of the central sub-array elements, N_s, can be expressed as:

$$\text{Central subarray} = \left\{\left(x_i, y_i\right), w_i\right\}_{i=1}^{N_s}, \tag{9}$$

while each of the surrounded ring elements has polar coordinate $\left(r_j, \varnothing_j\right)$ and its cartesian coordinate is:

$$x_j = r_j \cos\left(\varnothing_j\right), \quad y_j = r_j \sin\left(\varnothing_j\right). \tag{10}$$

These array elements are with complex weight excitation as:

$$w_j = a_j e^{j\psi_j}, \tag{11}$$

where a_j is amplitude and ψ_j is phase excitations.

Then, the optimization variables are:

$$u = \left\{r_j, \varnothing_j, a_j, \psi_j\right\} \text{ for } j = 1, 2, \ldots, N_r, \tag{12}$$

where N_r is the total number of surrounded elements in the circular ring region.

The optimization problem for such hybrid array is to minimize the PSL as follows:

$$\min_u \text{PSL}(u). \tag{13}$$

Under the constraints:

$$r_{\min} \le r_j \le r_{\max}, \ 0 \le a_j \le 1, \ \text{and} - \pi \le \varnothing_j \le \pi, \tag{14}$$

where the element positions are restricted within minimum and maximum specific bound within the required ring regions. Thus, the element positions in the ring region are only optimized, while the amplitude excitations are set to ones and the phase excitation are set to zeros.

4 Simulation results

4.1 Results of discrete hexagonal-based amplitude excitations

For the discrete hexagonal-based amplitude excitations, the author use an aperture radius $R_m = 4\lambda$, $d = 0.5\lambda$, and $\beta \in [0,10]$. The number of elements in each hexagonal ring R_m was determined by the optimizer. For the genetic optimization, the author used the build in function called "fmincon" with population size of 200 and maximum number of iteration equal to 400. The least square regularization parameter was set to $\lambda_r = 1e^{-2}$.

In the first example, the value of β was set to 0, thus, the discrete hexagonal-based amplitude excitations were uniform (i.e., unit amplitudes) and the corresponding array pattern has relatively high sidelobe level equal to −13.2 dB (see Fig. 3). In the second example, the β = 2.11 and the

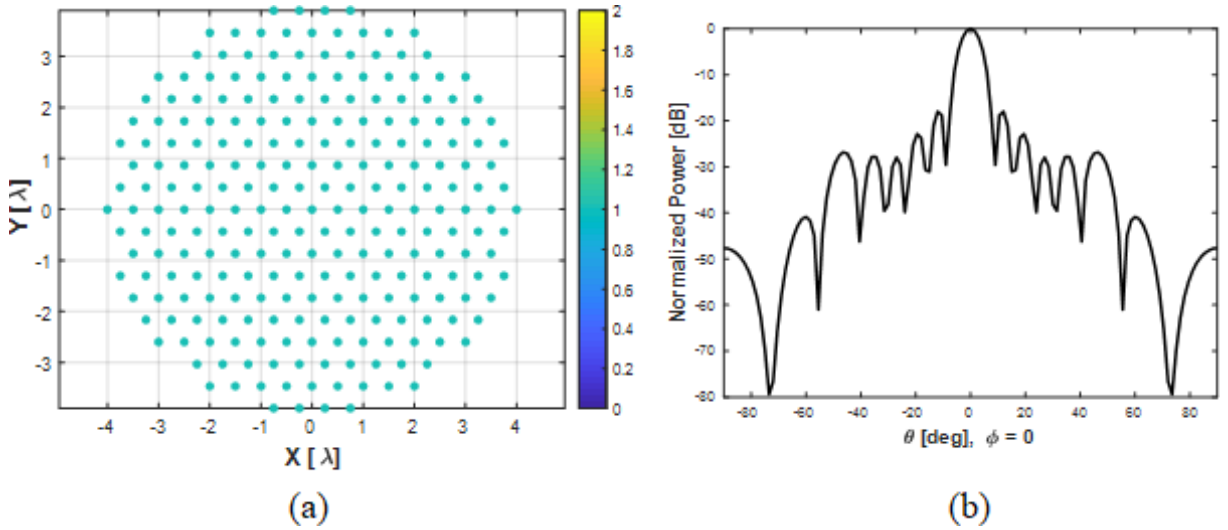

Fig. 3 Hexagonal ring-based amplitude excitations (a), and its corresponding array pattern (b) for $\beta = 0$, $R_m = 4\lambda$

discrete hexagonal-based amplitude excitation becomes quite clear and the corresponding array pattern has peak SLL = −20 dB (see Fig. 4). In the next example, $\beta = 5.65$ and the peak SLL was reduced to more than −45 dB (see Fig. 5). The array pattern and its corresponding discrete hexagonal-based amplitude excitations for $\beta = 5.65$, and $R_m = 8\lambda$ is shown in Fig. 6. All of these results fully confirm that the discrete hexagonal-based amplitude excitations approach can provide array patterns with minimized PSL. Compared to Dolph–Chebyshev or Taylor tapers, the proposed discrete hexagonal-based amplitude excitations method preserved narrower beamwidth while achieving additional sidelobe suppression.

4.2 Results of hybrid planar array

In the second proposed hybrid array, the size of the central sub-array was $N \times M = 8 \times 8$ elements, the inter-element spacing inside the central sub-array was $d = 0.5\lambda$ along both x- and y-axis, The total number of the surrounding elements is chosen to be 200 elements, the minimum allowed spacing between any two elements of these surrounded elements was constrained to $d_s = 0.6\lambda$, the inner and outer radius of the surrounded rings were 2.5λ and 6.0λ, respectively. The amplitude excitations of the central sub-array as well as the surrounded elements were fixed to uniform. Only the positions of the surrounded elements were optimized to get a minimum PSL according to Eqs. (13) and (14). The results are shown in Fig. 7 and Fig. 8 where the PSL was −20 dB. Note that further reduction in the peak SLL can be obtained with optimization of both element positions and excitations. However, there will be an increase in the feeding network complexity when optimizing the element excitations. Fig. 9 shows the results of a central subarray structure with surrounded elements that are arranged along a specific number of rings. Compare the results of Fig. 9 with that of Fig. 7;

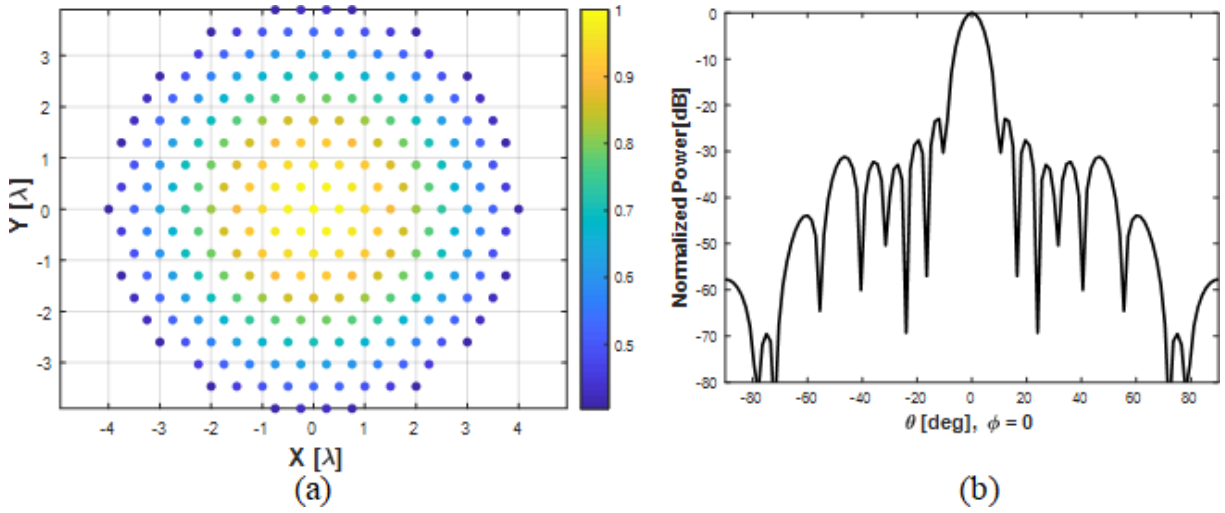

Fig. 4 Hexagonal ring-based amplitude excitations (a), and its corresponding array pattern (b) for $\beta = 2.11$, $R_m = 4\lambda$

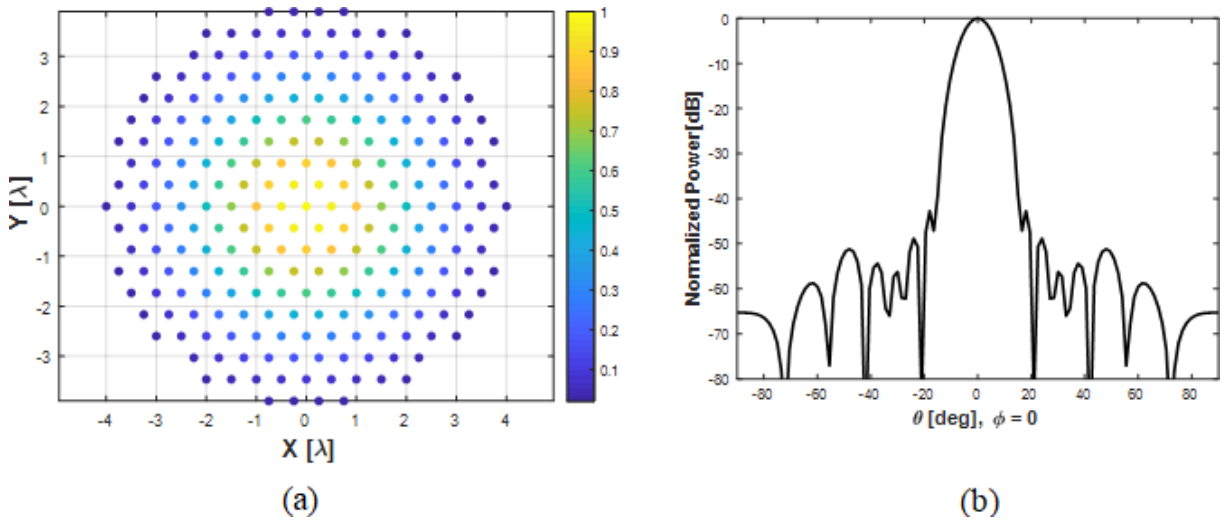

Fig. 5 Hexagonal ring-based amplitude excitations (a), and its corresponding array pattern (b) for $\beta = 5.65$, $R_m = 4\lambda$

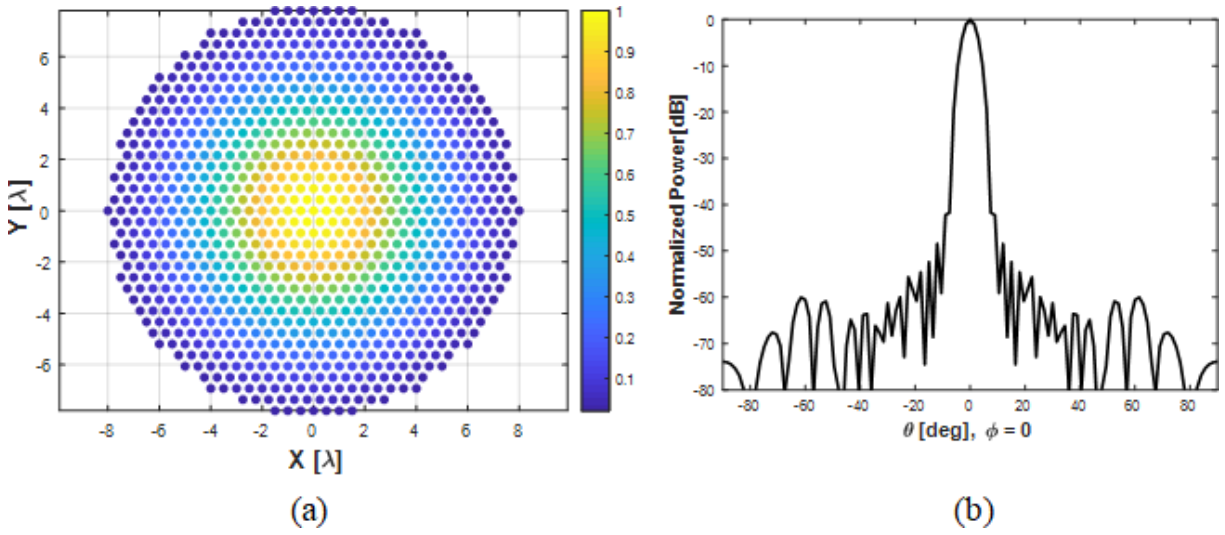

Fig. 6 Hexagonal ring-based amplitude excitations (a), and its corresponding array pattern (b) for $\beta = 5.65$, $R_m = 8\lambda$

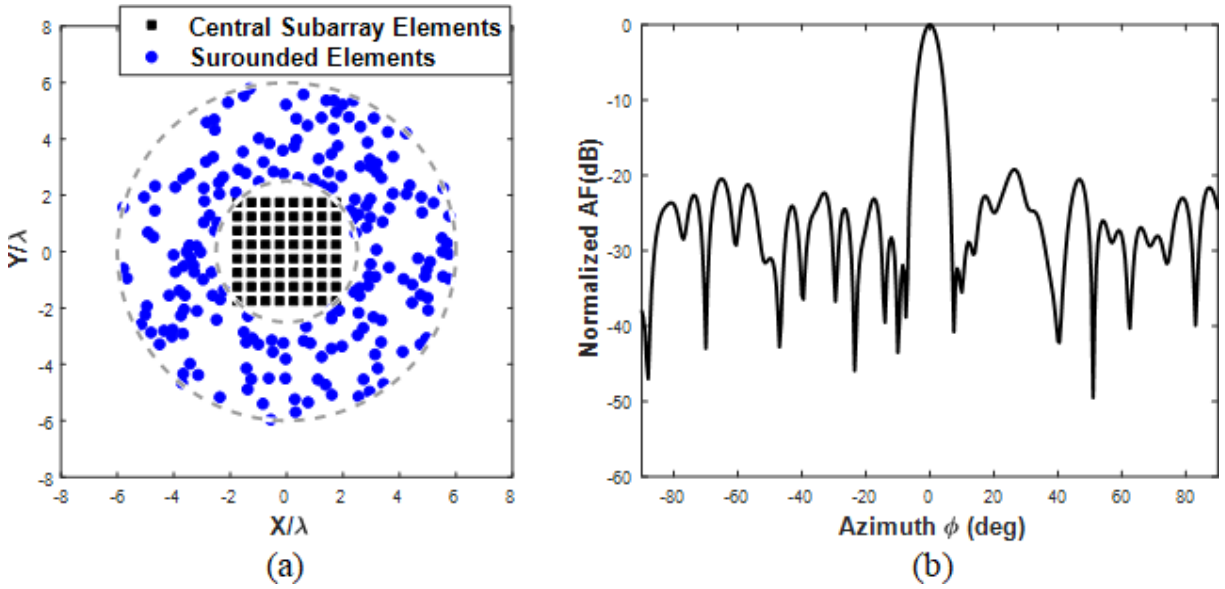

Fig. 7 Hybrid planar array geometry (a), and its corresponding array pattern (b) for position–only optimization and uniform amplitude excitations

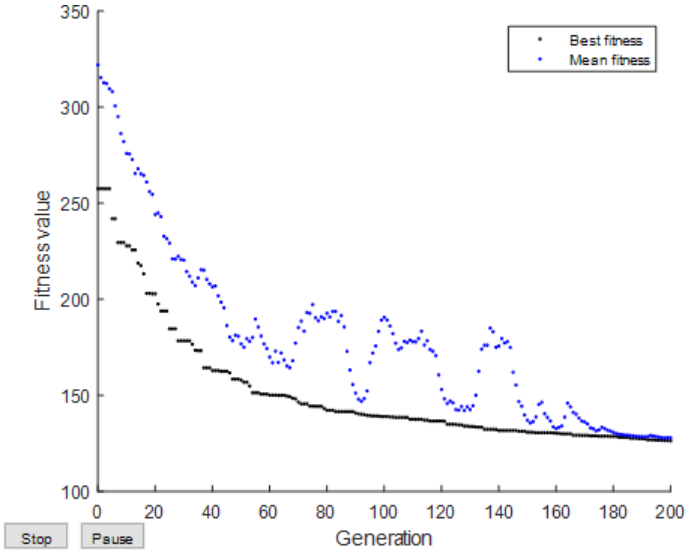

Fig. 8 Cost function variation of the hybrid planar array

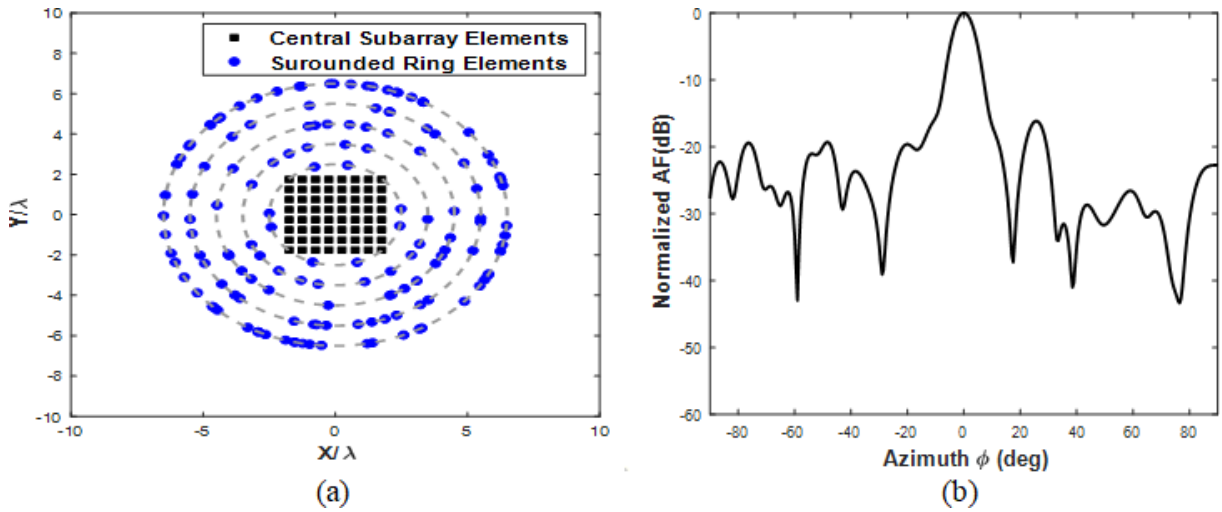

Fig. 9 Hybrid planar array geometry with circular rings (a), and its corresponding array pattern (b) for position–only optimization and uniform amplitude excitations

it is clear that the surrounded elements along the rings give an array patter with higher PSL about −17 dB than the previous case. This is mainly due to enforce more constraints on the array elements.

5 Conclusions

It was introduced a discrete hexagonal-based array pattern synthesized method for obtaining low sidelobes. Its design parameters were optimized by means of coupled GA and convex least square method. The designed hexagonal array has −45 dB sidelobes with controllable beamwidth under strict constraint value of $\beta = 5.65$. It is found that the first proposed method provides a balance between analytical simplicity and optimization flexibility.

Moreover, the proposed hexagonal array produces a low sidelobe level with monotonic decay, which is often preferred in radar and sonar applications. The practical implementation of the designed discrete hexagonal array is simpler and it can be easily and efficiently integrated with real-life discrete RF components such as digital attenuators. For electronically scanned arrays, the value of β can be reduced as scan angle increases. This helps to limit main beam broadening.

For the second proposed method, the designed hybrid array with surrounded element positions-control achieves a sidelobe level about −20 dB. Better results could be obtained with optimized element excitations and positions controls simultaneously.

References

[1] Vescovo, R., Pajewski, L. "Multiple-ring Circular Array for Ground-Penetrating Radar Applications: Basic Ideas and Preliminary Results", Journal of Telecommunications and Information Technology, 3, pp. 25–29, 2017. [online] Available at: https://iris.uniroma1.it/retrieve/e383531a-301c-15e8-e053-a505fe0a3de9/Vescovo_Multiple-ring_2017.pdf [Accessed: 10 September 2025]

[2] Yektakhah, B., Nasr, A. M. H., Mohamed, A. H., Sarabandi, K. "Low-Complexity Wideband Circularly Polarized Modular Scalable Phased Array for Vehicular Satellite Communication", IEEE Open Journal of Antennas and Propagation, 6(3), pp. 854–863, 2025. https://doi.org/10.1109/OJAP.2025.3551624

[3] Blomberg, A. E. A., Austeng, A., Hansen, R. E. "Adaptive Beamforming Applied to a Cylindrical Sonar Array Using an Interpolated Array Transformation", IEEE Journal of Oceanic Engineering, 37(1), pp. 25–34, 2012. https://doi.org/10.1109/JOE.2011.2169611

[4] Mohammed, J. R. "A New Simple Adaptive Noise Cancellation Scheme Based On ALE and NLMS Filter", In: Fifth Annual Conference on Communication Networks and Services Research (CNSR ,07), Fredericton, NB, Canada, 2007, pp. 245–254. ISBN 0-7695-2835-X https://doi.org/10.1109/CNSR.2007.4

[5] Mohammed, J. R., Singh, G. "An Efficient RLS Algorithm For Output-Error Adaptive IIR Filtering And Its Application To Acoustic Echo Cancellation", In: 2007 IEEE Symposium on Computational Intelligence in Image and Signal Processing, Honolulu, HI, USA, 2007, pp. 139–145. ISBN 1-4244-0707-9 https://doi.org/10.1109/CIISP.2007.369307

[6] Mohammed, J. R. "Low Complexity Adaptive Noise Canceller for Mobile Phones Based Remote Health Monitoring", International Journal of Electrical and Computer Engineering (IJECE), 4(3), pp. 422–432, 2014. https://doi.org/10.11591/ijece.v4i3.5534

[7] Kaiser, J. F. "Nonrecursive digital filter design using the I0-sinh window function", In: Proceedings of IEEE International Symposium on Circuits and Systems, San Francisco, CA, USA, 1974, pp. 20–23.

[8] Xiong, Z.-Y., Xu, Z.-H., Chen, S.-W., Xiao, S.-P. "Subarray Partition in Array Antenna Based on the Algorithm X", IEEE Antennas and Wireless Propagation Letters, 12, pp. 906–909, 2013. https://doi.org/10.1109/LAWP.2013.2272793

[9] Mohammed, J. R. "Rectangular Grid Antennas with Various Boundary Square-Rings Array", Progress In Electromagnetics Research Letters, 96, pp. 27–36, 2021. https://doi.org/10.2528/PIERL20112402

[10] Keizer, W. P. M. N. "Synthesis of Thinned Planar Circular and Square Arrays Using Density Tapering", IEEE Transactions on Antennas and Propagation, 62(4), pp. 1555–1563, 2014. https://doi.org/10.1109/TAP.2013.2267194

[11] Mohammed, J. R. "Simplified Rectangular Planar Array with Circular Boundary for Side lobe Suppression", Progress In Electromagnetics Research M, 97, pp. 57–68, 2020. https://doi.org/10.2528/PIERM20062906

[12] Mohammed, J. R. "Unconventional Method for Antenna Array Synthesizing Based on Ascending Clustered Rings", Progress In Electromagnetics Research Letters, 117, pp. 69–73, 2024. https://doi.org/10.2528/PIERL23122201

[13] Haupt, R. P. "Antenna Arrays: A Computational Approach", John Wiley & Sons, Inc., 2010. ISBN 9780470407752 https://doi.org/10.1002/9780470937464

[14] Mohammed, J. R. "Synthesizing Non-Uniform Antenna Arrays Using Tiled Subarray Blocks", Journal of Telecommunications and Information Technology, 4, pp. 25–29, 2023. https://doi.org/10.26636/jtit.2023.4.1417

[15] Mohammed, E. A., Mohammed, J. R. "Improving the Radiation Characteristics of the Tapered Window Functions Using Partially Unit Amplitude Constraints", International Journal of Microwave and Optical Technology, 20(1), pp. 54–62, 2025. [online] Available at: https://www.researchgate.net/publication/393430935_Improving_the_Radiation_Characteristics_of_the_Tapered_Window_Functions_Using_Partially_Unit_Amplitude_Constraints [Accessed: 10 September 2025]

[16] Abdulqader, A. J., Mohammed, J. R., Ali, Y. A. "A T-Shaped Polyomino Subarray Design Method for Controlling Sidelobe Level", Progress In Electromagnetics Research C, 126, pp. 243–251, 2022. https://doi.org/10.2528/PIERC22080803

[17] Mohammed, J. R., Abdulqader, A. J., Thaher, R. H. "Array Pattern Recovery under Amplitude Excitation Errors Using Clustered Elements", Progress In Electromagnetics Research M, 98, pp. 183–192, 2020. https://doi.org/10.2528/PIERM20101906

[18] Mohammed, J. R., Sayidmarie, K. H. "Sensitivity of the Adaptive Nulling to Random Errors in Amplitude and Phase Excitations in Array Elements", Journal of Telecommunication, Electronic and Computer Engineering (JTEC), 10(1), pp. 51–56, 2018. [online] Available at: https://jtec.utem.edu.my/jtec/article/view/2023 [Accessed: 10 September 2025]

[19] Mohammed, J. R. "An optimum side-lobe reduction method with weight perturbation", Journal of Computational Electronics, 18(2), pp. 705–711, 2019. https://doi.org/10.1007/s10825-019-01323-5

[20] Balanis, C. A. "Antenna Theory: Analysis and Design", John Wiley & Sons, Inc., 2005. ISBN 0-471-66782-X [online] Available at: https://ia800501.us.archive.org/30/items/AntennaTheoryAnalysisAndDesign3rdEd/Antenna%20Theory%20Analysis%20and%20Design%203rd%20ed.pdf [Accessed: 10 September 2025]